Heliyon 9 (2023) e20180

Contents lists available at ScienceDirect

Heliyon

journal homepage: www.cell.com/heliyon

Role of multiple dual-phase ^{18}F-FDG PET/CT metabolic parameters in differentiating adenocarcinomas from squamous cell carcinomas of the lung

Xue Liu [1], Qiao Zou [1], Yu Sun, Huiting Liu, Gao Cailiang [*]

Department of Nuclear Medicine, Chongqing University Three Gorges Hospital, Wanzhou, 404100, Chongqing, China

ARTICLE INFO

Keywords:
NSCLC
Adenocarcinoma
Squamous cell carcinoma
PET/CT
Dual-phase

ABSTRACT

Purpose: To evaluate the ability of multiple dual-phase ^{18}F-fluorodeoxyglucose positron emission tomography/computed tomography (^{18}F-FDG PET/CT) metabolic parameters to distinguish the histological subtypes of non-small cell lung cancer (NSCLC).

Methods: Data from 127 patients with non-small cell lung cancer who underwent preoperative dual-phase ^{18}F-FDG PET/CT scanning at the PET-CT center of our hospital from December 2020 to October 2021 were collected, and the metabolic parameters of their primary lesions were measured and analyzed retrospectively. Intraclass correlation coefficients (ICC) were calculated for consistency between readers. Metabolic parameters in the early (SUV_{peak}, SUV_{mean}, SUV_{min}, SUV_{max}, MTV, and TLG) and delayed phases ($dpSUV_{peak}$, $dpSUV_{mean}$, $dpSUV_{min}$, $dpSUV_{max}$, dpMTV, and dpTLG) were calculated. We drew receiver operating characteristic (ROC) curves to compare the differences in different metabolic parameters between the adenocarcinoma (AC) and squamous cell carcinoma (SCC) groups and evaluated the ability of different metabolic parameters to distinguish AC from SCC.

Results: Inter-reader agreement, as assessed by the intraclass correlation coefficient (ICC), was good (ICC = 0.71, 95% CI:0.60–0.79). The mean MTV, SUV_{max}, TLG, SUV_{peak}, SUV_{mean}, $dpSUV_{max}$, dpTLG, $dpSUV_{peak}$, $dpSUV_{mean}$, and $dpSUV_{min}$ of the tumors were significantly higher in SCC lesions than in AC lesions ($P = 0.049$, < 0.001, 0.016, < 0.001, 0.001, < 0.001, 0.018, < 0.001, 0.001, and 0.001, respectively). The diagnostic efficacy of the metabolic parameters in ^{18}F-FDG PET/CT for differentiating adenocarcinoma from squamous cell carcinoma ranged from high to low as follows: SUV_{peak} (AUC = 0.727), SUV_{max} (AUC = 0.708), $dpSUV_{max}$ (AUC = 0.699), $dpSUV_{peak}$ (AUC = 0.698), TLG (AUC = 0.695), and dpTLG (AUC = 0.692), SUV_{mean} (AUC = 0.690), $dpSUV_{mean}$ (AUC = 0.687), $dpSUV_{min}$ (AUC = 0.680), SUV_{min} (AUC = 0.676), and MTV (AUC = 0.657).

Conclusions: Squamous cell carcinoma of the lung had higher mean MTV, SUV_{max}, TLG, SUV_{peak}, SUV_{mean}, SUV_{min}, $dpSUV_{peak}$, $dpSUV_{mean}$, $dpSUV_{min}$, $dpSUV_{max}$, and dpTLG than AC, which can be helpful tools in differentiating between the two. The metabolic parameters of the delayed phase (2 h after injection) ^{18}F-FDG PET/CT did not improve the diagnostic efficacy in distinguishing lung AC from SCC. Conventional dual-phase ^{18}F-FDG PET/CT is not recommended.

* Corresponding author.
E-mail address: 18315025386@163.com (G. Cailiang).
[1] Xue Liu, Qiao Zou contributed to the work equally and should be regarded as co-first authors.

https://doi.org/10.1016/j.heliyon.2023.e20180
Received 12 April 2023; Received in revised form 6 September 2023; Accepted 13 September 2023
Available online 21 September 2023
2405-8440/© 2023 The Authors. Published by Elsevier Ltd. This is an open access article under the CC BY-NC-ND license (http://creativecommons.org/licenses/by-nc-nd/4.0/).

1. Introduction

Lung cancer is the most prevalent thoracic malignancy. In 2020, the latest global cancer statistics released by the International Agency for Research on Cancer of the World Health Organization showed that lung cancer ranks second in global incidence after breast cancer and is the leading cause of cancer-related death [1,2]. Lung cancer is a highly heterogeneous malignant epithelial tumor with distinct pathological features and clinical behavior [3]. Non-small-cell lung cancer (NSCLC) is the most common type of lung cancer, with subtypes such as adenocarcinoma, squamous cell carcinoma, and large-cell carcinoma [3]. The optimal management of NSCLC depends on factors such as the histological subtype, molecular characteristics, and tumor stage [4]. Scagliotti et al. found that compared with docetaxel, pemetrexed significantly prolonged adenocarcinoma's (AC) overall survival and progression-free survival but had the opposite effect on squamous cell carcinoma (SCC) [5]. Additionally, bevacizumab, used in treating patients with AC, is contraindicated for those with SCC [6]. To select appropriate targeted drugs to prolong the survival of patients with lung cancer, it is essential to determine the pathological type [6].

Pathology remains the gold standard for diagnosing histological subtypes of lung cancer; however, the diagnosis of pathological subtypes remains unclear for many patients for various reasons, such as the special location of the lesion, invasive examination, and ineffective puncture [7]. ^{18}F-Fluorodeoxyglucose positron emission tomography/computed tomography (^{18}F-FDG PET/CT) is a noninvasive imaging modality that plays important roles in tumor diagnosis, staging, restaging, radiotherapy planning, and therapy monitoring [8].

As the uptake of ^{18}F-FDG reflects the metabolic rate of living tumor cells, it can reflect both the invasive and pathological types of tumors [9]. Single-time-point ^{18}F-FDG PET lacks dynamic information regarding ^{18}F-FDG accumulation in a lesion and sometimes shows metabolic parameter overlap between malignant and benign lesions. To improve the accuracy of ^{18}F-FDG PET for differentiating benign from malignant lesions, dual-phase ^{18}F-FDG PET was proposed. The theoretical basis for this is that the FDG uptake by different cells changes differently over time [10]. Dual-phase FDG PET has been reported to have the potential to improve the accuracy of evaluating lung nodules, with only borderline levels of increased metabolic activity [11]. Some studies [12,13] support this hypothesis and achieved similar results using dual-phase ^{18}F-FDG-PET scanning. Recent research has focused on using PET/CT in the diagnosis, staging, and follow-up of patients and differentiating between different histological subtypes and tumor grades [14,15].

Multiple dual-phase ^{18}F-FDG PET/CT metabolic parameters reflect the lesion metabolic activity and can be easily calculated. Several well-known parameters are used to distinguish between malignant and benign lesions [9,16] and predict the prognosis of patients with lung cancer [17]. Many previous studies have shown that the maximum standardized uptake value (SUVmax) of the primary lesion on PET/CT correlates with tumor malignancy and prognosis after therapy [18,19]. However, to the best of our knowledge, few studies have evaluated the use of dual-phase ^{18}F-FDG PET/CT and different metabolic parameters to differentiate the NSCLC subtypes.

Therefore, we measured various metabolic parameters for primary lung cancer in dual-phase ^{18}F-FDG PET/CT examinations in the early and delayed phases. We compared the diagnostic abilities of different metabolic parameters in distinguishing AC from SCC and evaluated the noninvasive differentiation of NSCLC subtypes using dual-phase ^{18}F-FDG PET/CT.

2. Materials and methods

2.1. Patient selection

This study was retrospective and was approved by the academic ethics committee of Chongqing University Three Gorges Hospital (Ethics No. CQUTGH-202096). We collected data from patients with lung tumors who underwent whole-body PET/CT examination at our hospital's PET/CT center between December 2020 and October 2021.

The inclusion criteria were as follows: (1) a biphasic PET/CT systemic examination was performed, and the PET/CT image data were complete, clear, and capable of outlining the corresponding region of interest. (2) Pathological confirmation of adenocarcinoma or squamous cell carcinoma using computed tomography-guided puncture, ultrasound-guided puncture, or surgery. (3) No radiotherapy, chemotherapy, or other treatment was administered before the scan. (4) No age or sex restrictions were not imposed.

The exclusion criteria were as follows: (1) patients with pathological types of small cell carcinoma or other types of non-small cell carcinoma and (2) lesions that were too numerous or too large to accurately outline the Region of interest (ROI).

2.2. PET/CT imaging

Imaging data were acquired using a hybrid PET/CT scanner (uMI780, United Imaging, China) 1 h after the intravenous injection of ^{18}F-FDG. Before the examination, each patient fasted for more than 6 h and had a blood glucose level of less than 8.6 mmol/L measured by fingertip blood sampling. The dose of ^{18}F-FDG was based on the patient's body weight (0.11–0.14 mCi/kg). The patients rested quietly after the injection. ^{18}F-FDG was produced and supplied by Atomic Hi-Tech Co., Ltd., with a pH value of 5–7 and a radiochemical purity of over 95%. Sixty minutes later, whole-body scanning was performed from the head to the upper thigh. The ordered subset expectation maximization (OSEM) iterative method was used for PET image reconstruction. The CT parameters were as follows: tube voltage, 120 kV; tube current, 140 mA; and slice thickness, 3.75 mm. A PET scan immediately followed the CT scan in 3D acquisition mode with six–eight bed positions and two-and-a-half minutes per position. Attenuation correction of the PET images was performed using CT data. PET/CT images obtained 1 h after injection were defined as the early phase. An additional delayed scan of the

lung lesion area was performed 2 h after the injection using the same scanner. The images acquired during this time were in the delayed phase.

For interpretation, attenuation-corrected ^{18}F-FDG PET, CT, and fused PET/CT images were displayed in transverse, coronal, and sagittal views as rotating maximum-intensity projection images.

2.3. Postprocessing of ^{18}f-FDG-PET/CT images

Two experienced nuclear medicine physicians interpreted and analyzed all the images using available clinical information. Any disagreements were discussed, and a consensus was reached. They viewed the fused PET/CT images on a dedicated workstation (UMI-WS with a PET/CT viewer for automated image registration). They drew a region of interest (ROI) on a transaxial image around each primary tumor lesion for semiquantitative analysis. The software automatically calculates the peak standardized uptake value (SUV_{peak}), mean standardized uptake value (SUV_{mean}), minimum standardized uptake value (SUV_{min}), maximum standardized uptake value (SUV_{max}), metabolic tumor volume (MTV), and total lesion glycolysis (TLG). They expressed early early-phase (1 h after injection) semiquantitative metabolic parameters, such as SUV_{peak}, SUV_{mean}, SUV_{min}, SUV_{max}, MTV, and TLG. They expressed delayed-phase (2 h after injection) semiquantitative metabolic parameters such as $dpSUV_{peak}$, $dpSUV_{mean}$, $dpSUV_{min}$, $dpSUV_{max}$, dpMTV, and dpTLG.

2.4. Statistical analysis

We calculated the intraclass correlation coefficients (ICC) to assess the consistency between the two readers (XL and QZ). We classified ICCs as follows:0.00–0.20, poor agreement; 0.21–0.40, fair agreement; 0.41–0.60, moderate agreement; 0.61–0.80, good agreement; and 0.81–1.00, excellent agreement. We described measurement data with a normal distribution using mean ± standard deviation and compared groups using independent samples *t* tests. We described measurements that did not follow a normal distribution with medians (lower quartiles and upper quartiles) [M (P25, P75)] and compared the groups using the Mann−Whitney *U* test. We described the enumeration data as the number of cases (percentage) and compared the groups using the chi-squared test or Fisher's exact probability method. We used ROC and AUC to evaluate the diagnostic efficacy of FDG PET/CT metabolic parameters in identifying the pathological subtypes of non-small cell carcinoma and to determine the optimal diagnostic threshold. Spearman's rank correlation analysis was used to evaluate the correlation between FDG PET/CT metabolic parameters and pathological subtypes. $|rs| < 0.4$ indicated low correlation, $0.4 < |rs| < 0.7$ indicated moderate correlation; $|rs| > 0.7$ indicated high correlation: $rs > 0$, positive correlation; $rs < 0$, negative correlation. We considered two-tailed *P*-values < 0.05. We performed an FDR correction on the *P* value to control the number of false positives. We used SPSS 25.0 (version 23.0; SPSS, Chicago, IL, USA) and R language software for statistical analysis or graphics.

3. Results

3.1. Patient characteristics

We included 127 patients with NSCLC based on inclusion and exclusion criteria. Of these, 97 (75.38%) were male, and 30 (23.62%) were female, with a mean age of 63.11 ± 9.19 years and 62.30 ± 8.85 years, respectively. The pathological types were AC in 76 patients (59.84%) and SCC in 51 patients (40.16%). Of the patients with AC, 46 (60.53%) were male, and 30 (39.47%) were female; all patients with SCC were male. The sex ratio differed significantly between the AC and SCC groups (*P* value < 0.001) by the X^2 or Fisher's exact test. There were no significant differences in age, body weight, blood glucose level, or ^{18}F-FDG dose between groups. However,

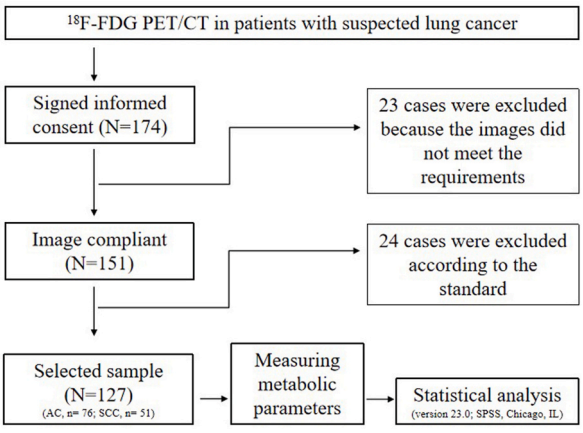

Fig. 1. Flow chart summarizing eligibility/exclusion criteria for the final study population.

the lesion size was larger in the SCC group than in the AC group ($P < 0.01$). Fig. 1 illustrates the study design. Table 1 presents the demographic and clinical characteristics of the AC and SCC cohort.

3.2. Metabolic parameters of PET/CT

The ICC for the inter-reader agreement was 0.86 between readers 1 (XL) and 2 (QZ) ($P < 0.05$). All lesions had higher metabolic parameter values in the delayed phase than in the conventional phase ($P < 0.05$). The mean MTV and TLG for all primary tumor sites were 32.82 ± 43.66 and 203.72 ± 289.00, respectively. Squamous cell carcinomas had higher MTV and TLG values than adenocarcinomas ($P < 0.05$). The mean SUV_{max}, SUV_{min}, $SUV_{mean,}$ and SUV_{peak} of all primary tumors were 10.68 ± 4.59, 3.23 ± 1.2, 5.70 ± 2.32, and 8.52 ± 3.84, respectively; these values were significantly higher for squamous cell carcinoma than for adenocarcinoma (all $P < 0.001$). The mean $dpSUV_{max}$, $dpSUV_{min}$, $dpSUV_{mean,}$ and $dpSUV_{peak}$ for all primary tumors were 13.53 ± 5.54, 4.01 ± 1.56, 7.04 ± 2.90, and 10.94 ± 4.40, respectively; these values were also significantly higher for squamous cell carcinoma than for adenocarcinoma (all $P < 0.001$). The mean dpTLG for all primary tumors was 226.49 ± 319.14; it was significantly higher for squamous cell carcinoma (311.88 ± 355.37) than for adenocarcinoma (169.18 ± 280.41) ($P = 0.018$). The mean dpMTV for all primary tumors was 30.39 ± 39.42; there was no significant difference in dpMTV between squamous cell carcinoma and adenocarcinoma ($P = 0.068$) [Fig. 2(A–E) and Fig. 3(A–E)].

3.3. Correlations between metabolic indicators

Our study found a significant correlation between these metabolic parameters and the pathological types; however, this correlation was mild ($r_s < 0.4$, all $P < 0.01$). The MTV was moderately positively correlated with SUV_{max}, SUV_{peak}, SUV_{mean}, SUV_{min}, $dpSUV_{max}$, and $dpSUV_{peak}$. The MTV was positively correlated with $dpSUV_{mean}$ and $dpSUV_{min}$. SUV_{max} was highly positively correlated with SUV_{peak}, SUV_{mean}, SUV_{min}, $dpSUV_{max}$, $dpSUV_{peak}$, $dpSUV_{mean}$, and $dpSUV_{min}$; moderately positively correlated with TLG; and weakly positively correlated with dpMTV. The TLG was highly positively correlated with dpMTV and moderately positively correlated with SUV_{peak}, SUV_{mean}, SUV_{min}, $dpSUV_{max}$, $dpSUV_{peak}$, $dpSUV_{mean}$, and $dpSUV_{min}$. SUV_{peak} was highly positively correlated with SUV_{mean}, SUV_{min}, $dpSUV_{max}$, $dpSUV_{peak}$, $dpSUV_{mean}$, and $dpSUV_{min}$ and moderately positively correlated with dpMTV. SUV_{mean} was highly positively correlated with SUV_{min}, $dpSUV_{max}$, $dpSUV_{peak}$, $dpSUV_{mean}$, and $dpSUV_{min}$ and weakly positively correlated with dpMTV. SUV_{min} was highly positively correlated with $dpSUV_{max}$, $dpSUV_{peak}$, $dpSUV_{mean}$, and $dpSUV_{min}$ and slightly positively correlated with dpMTV. dpMTV showed a low positive correlation with $dpSUV_{max}$ $dpSUV_{peak}$ $dpSUV_{mean}$ $dpSUV_{min}$. The $dpSUV_{max}$ was highly positively correlated with the $dpSUV_{peak}$, $dpSUV_{mean}$, and $dpSUV_{min}$. The $dpSUV_{peak}$ was highly positively correlated with the $dpSUV_{mean}$ and $dpSUV_{min}$. $dpSUV_{mean}$ was highly positively correlated with dpSUVmin. The correlation coefficients are shown in Fig. 4.

Table 1
Patient characteristics.

Characteristics	Overall	AC	SCC	X^2/t	P
Sex (male/female)	97/30	46/30	51/0	48.399	< 0.001
Age (years)	62.92 ± 9.09	61.66 ± 8.89	64.80 ± 9.13	−1.934	0.055
Smoking (Yes/No)	56/71	38/38	18/33	2.677	0.102
Drinking (Yes/No)	81/46	53/23	28/23	2.907	0.088
Weight (kg)	58.23 ± 9.14	57.54 ± 10.19	59.26 ± 7.27	−1.044	0.298
Blood glucose (mmol/L)	5.22 ± 0.93	5.29 ± 0.94	5.12 ± 0.91	1.028	0.306
^{18}F-FDG (mCi)	7.56 ± 1.20	7.40 ± 1.26	7.80 ± 1.08	−1.895	0.060
Long Axis	40.92 ± 17.16	36.97 ± 14.54	46.81 ± 19.14	−3.289	0.001
Short Axis	26.39 ± 12.68	23.86 ± 12.19	30.15 ± 12.57	−2.817	0.006
MTV	32.82 ± 43.66	26.58 ± 41.09	42.13 ± 46.08	−1.991	0.049
TLG	203.72 ± 289.00	151.25 ± 255.97	281.89 ± 319.03	−2.444	0.016
SUV_{max}	10.68 ± 4.59	9.43 ± 4.11	12.55 ± 4.67	−3.963	< 0.001
SUV_{peak}	8.52 ± 3.84	7.32 ± 3.48	10.52 ± 3.76	−4.282	< 0.001
SUV_{mean}	5.70 ± 2.32	5.12 ± 2.14	6.58 ± 2.32	−3.645	< 0.001
SUV_{min}	3.23 ± 1.24	3.03 ± 1.15	3.76 ± 1.25	−3.387	0.001
dpMTV	30.39 ± 39.42	25.16 ± 38.69	38.18 ± 39.57	−1.843	0.068
dpTLG	226.49 ± 319.14	169.18 ± 280.41	311.88 ± 355.37	−2.408	0.018
$dpSUV_{max}$	13.53 ± 5.54	12.07 ± 5.05	15.71 ± 5.56	−3.825	< 0.001
$dpSUV_{peak}$	10.94 ± 4.40	9.83 ± 4.20	12.61 ± 4.19	−3.657	< 0.001
$dpSUV_{mean}$	7.04 ± 2.90	6.34 ± 2.71	8.07 ± 2.88	−3.45	0.001
$dpSUV_{min}$	4.01 ± 1.56	3.65 ± 1.47	4.54 ± 1.54	−3.295	0.001

^{18}F-FDG.

^{18}F-fluorodeoxyglucose. MTV: metabolic volume of the tumor. TLG: total lesion glycolysis. SUV_{max}: maximum standardized uptake value. SUV_{peak}: peak standardized uptake value. SUV_{mean}: mean standardized uptake value. SUV_{min}: minimum standardized uptake value. dpMTV: MTV of the delayed phase. dpTLG: TLG of the delayed phase. $dpSUV_{max}$: SUV_{max} of the delayed phase. $dpSUV_{peak}$: SUV_{peak} of the delayed phase. $dpSUV_{mean}$: SUV_{mean} of the delayed phase. $dpSUV_{min}$: SUV_{min} of the delayed phase.

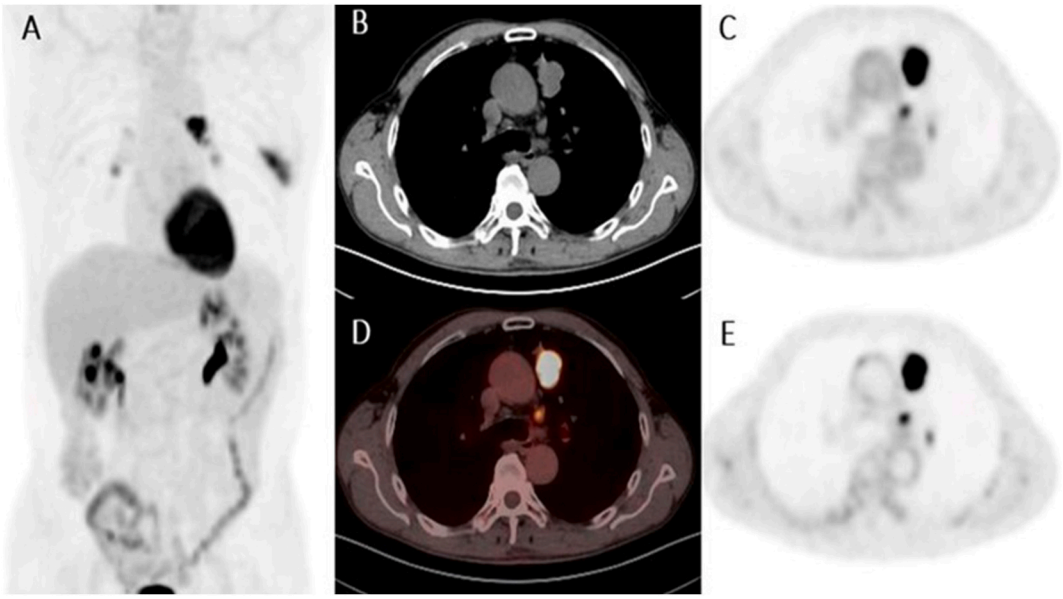

Fig. 2. A 58-year-old male patient proved histopathologically to have AC involving the left upper lobe. A, Whole body multiple intensity projection (MIP) image (upper). B, Axial CT in a mediastinal window. C, Axial early phase PET. D, Axial PET/CT images. E, Axial delayed phase PET. The SUV_{peak}, SUV_{mean}, SUV_{min}, SUV_{max}, MTV, and TLG of the tumor measured in the C image respectively was 11.02, 7.70, 4.39, 12.84, 9.05, and 69.71. The $dpSUV_{peak}$, $dpSUV_{mean}$, $dpSUV_{min}$, $dpSUV_{max}$, dpMTV, and dpTLG of the tumor measured in the E image respectively was 11.82, 8.42, 4.73, 13.47, 8.79, and 74.03.

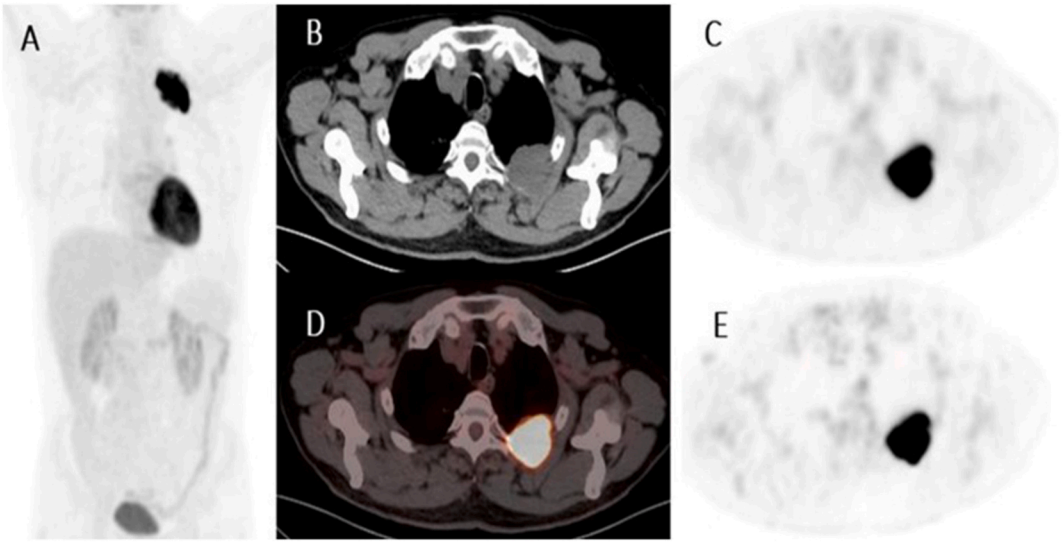

Fig. 3. A 64-year-old male patient proved histopathologically to have SCC involving the left upper lobe. A, Whole body multiple intensity projection (MIP) image (upper). B, Axial CT in a mediastinal window. C, Axial early phase PET. D, Axial PET/CT images. E, Axial delayed phase PET. The SUV_{peak}, SUV_{mean}, SUV_{min}, SUV_{max}, MTV, and TLG of the tumor measured in the C image respectively was 22.17, 11.76, 6.53, 26.39, 39.58, and 453.88. The $dpSUV_{peak}$, $dpSUV_{mean}$, $dpSUV_{min}$, $dpSUV_{max}$, dpMTV, and dpTLG of the tumor measured in the E image respectively was 21.75, 12.58, 6.88, 27.43, 36.88, and 463.96.

3.4. Diagnostic efficacy of metabolic parameters for AC and SCC

Among all metabolic indicators, SUV_{mean} had the highest sensitivity in the differential diagnosis of AC and SCC, with a cutoff value of 4.16 and a sensitivity of 0.902. However, the specificity was the lowest (0.395). $dpSUV_{peak}$ had the highest specificity in the differential diagnosis of AC and SCC, with a cutoff value of 12.14 and a sensitivity of 0.763; however, its sensitivity was the lowest, with a sensitivity of 0.569. By comparing the AUC of all metabolic indicators, we found that the value for SUV_{peak} was the highest at 0.727

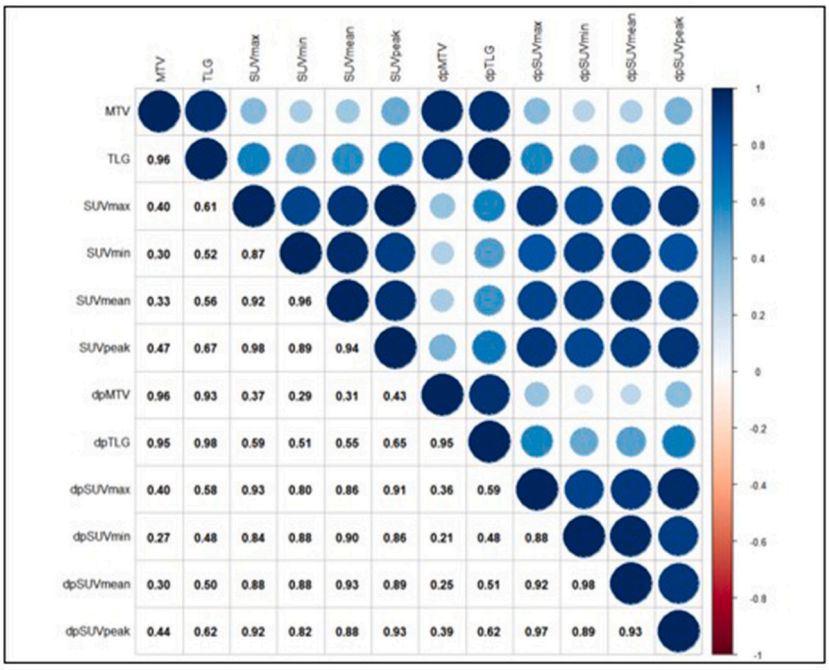

Fig. 4. Correlations analysis of between metabolic indicators.

(0.638–0.815), and the corresponding sensitivity and specificity were 0.745 and 0.658, respectively. The total AUCs of the other indicators were as follows: SUV_{max} (0.708); $dpSUV_{max}$ (0.699); $dpSUV_{peak}$ (0.698); TLG (0.695) dpTLG, (0.692); SUV_{mean} (0.690); $dpSUV_{mean}$ (0.687), $dpSUV_{min}$ (0.680), SUV_{min} (0.676), $dpSUV_{peak}$ (0.698), TLG (0.695), dpTLG (0.692), SUV_{mean} (0.687), $dpSUV_{min}$ (0.680), SUV_{min} (0.676); and MTV (0.657) (Table 2, Fig. 5).

4. Discussion

Lung cancer is one of the most common malignant tumors that endangers human health. In China and worldwide, lung cancer incidence and mortality are at the forefront and show an increasing trend each year [1,2]. With the increasing intensity of lung cancer screening in clinics, lung cancer incidence has also increased [1]. The precise treatment of NSCLC, such as the selection of targeted drugs, is closely related to the accuracy of pathological typing; however, invasive medical tests are not applicable to every patient and have limitations. Therefore, imaging modalities, especially ^{18}F-FDG PET/CT, are powerful complements to this [5]. There are few studies on the relationship between the pathological types of NSCLC and dual-phase ^{18}F-FDG PET/CT, and the conclusions differ [20].

As a noninvasive imaging technology, ^{18}F-FDG PET/CT not only provides morphological manifestations of lesions but also provides a variety of metabolic parameters, such as SUV, SUL, MTV, and TLG, to predict the pathological type of lung cancer by reflecting the metabolic activity of tumor cells, cell proliferation, and invasiveness through glucose metabolism [21,22]. Recent studies have demonstrated a significant correlation between metabolic parameters obtained through PET imaging and the pathological types of cancer [9]. For instance, patients with squamous cell carcinoma typically exhibit larger lesions than those with adenocarcinoma, which are statistically significant [9]. This may be because the expression of glucose transporters in lung squamous cell carcinoma is higher than that in adenocarcinoma, and the heterogeneity of squamous cell carcinoma is greater than that in other pathological types of lung cancer [23]. Squamous cell carcinomas proliferate faster, have shorter doubling times, and require more energy than adenocarcinoma cells [23]. Some studies [15,17] have shown that ^{18}F-FDG PET/CT has a high value in predicting the pathological type of lung cancer. Similar results were obtained in this study. There was a significant relationship between tumor histopathology and MTV, SUV_{max}, TLG, SUV_{peak}, SUV_{mean}, SUV_{min}, dpMTV, $dpSUV_{max}$, $dpSUV_{peak}$, $dpSUV_{mean}$ and $dpSUV_{min}$ (all P values < 0.01). MTV, SUV_{max}, TLG, SUV_{peak}, SUV_{mean}, SUV_{min}, dpMTV, $dpSUV_{peak}$, $dpSUV_{mean}$, dpSUV $_{min}$, dpSUV $_{max,}$ and dpTLG were higher in the squamous cell carcinoma group than in the adenocarcinoma group. Except for the difference in dpMTV between the two groups ($P =$ 0.018), the differences in other metabolic parameters were significant (all $P < 0.05$). The correlation between these metabolic parameters and the pathology was relatively weak; however, the correlation between each metabolic parameter was relatively strong. The weak correlation between metabolic parameters and pathology may be related to the fact that we only considered the effects of pathological type on metabolic parameters. In contrast, the effects of other factors (such as sex, tumor size, degree of pathological differentiation, and clinical stage) on metabolic parameters were not controlled. The correlation between various metabolic parameters was a relatively strong correlation between various metabolic parameters [9,24]. For example, SUV_{max} can be used to calculate MTV, and TLG is equal to the product of SUV_{mean} and MTV.

Table 2
Diagnostic efficacy of different metabolic parameters of^{18}–FDG PET/CT in AC and SCC.

Metabolic parameter	Cut-off value	Sensitivity	Specificity	Youden's index	AUC (95% CI)	*P*
MTV	10.29	0.784	0.500	0.284	0.657 (0.562–0.752)	0.003
SUV_{max}	10.10	0.706	0.658	0.360	0.708 (0.617–0.799)	< 0.001
TLG	57.28	0.824	0.513	0.337	0.695 (0.604–0.786)	< 0.001
SUV_{peak}	8.23	0.745	0.658	0.403	0.727 (0.638–0.815)	< 0.001
SUV_{mean}	4.16	0.902	0.395	0.297	0.690 (0.597–0.782)	< 0.001
SUV_{min}	2.84	0.784	0.487	0.271	0.676 (0.582–0.770)	0.001
$dpSUV_{max}$	13.37	0.667	0.697	0.364	0.699 (0.608–0.791)	< 0.001
dpTLG	83.65	0.765	0.579	0.344	0.692 (0.600–0.784)	< 0.001
$dpSUV_{peak}$	12.14	0.569	0.763	0.332	0.698 (0.607–0.790)	< 0.001
$dpSUV_{mean}$	7.26	0.608	0.711	0.318	0.687 (0.593–0.781)	< 0.001
$dpSUV_{min}$	3.25	0.824	0.487	0.310	0.680 (0.586–0.774)	0.001

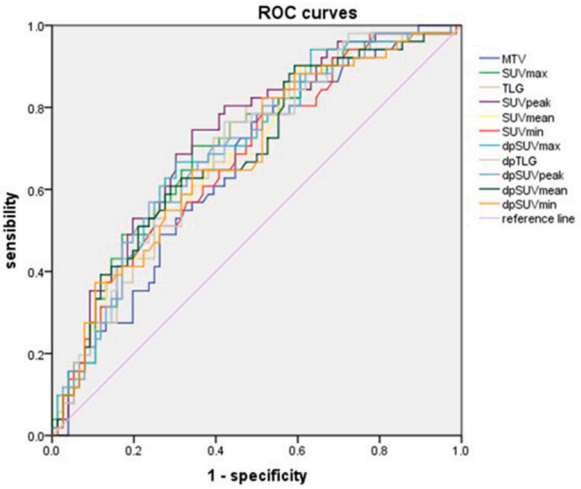

Fig. 5. ROC curve of the metabolic parameters concerning the histopathology of the lesion.

^{18}F-FDG PET can also provide dual-phase imaging according to different imaging times [25], thus improving diagnostic accuracy through delayed metabolic parameters of the lesion or changes in the lesion before and after the delay [26,27]. Our study found that the metabolic parameters in the delayed phase were higher than those in the conventional phase. The theoretical basis is that with a delay in time, the changing trends of ^{18}F-FDG uptake by different cells are different [28]. Studies [11,29] have suggested that dual-phase ^{18}F-FDG PET/CT can improve the diagnostic accuracy for benign and malignant lung lesions, has great clinical value, and is recommended for routine dual-phase ^{18}F-FDG PET/CT. However, some studies [30,31] have suggested that the diagnostic value of dual-phase ^{18}F-FDG PET/CT is limited and that conventional dual-phase ^{18}F-FDG PET/CT is not recommended for differential diagnoses. In this study, ROC curves of metabolic parameters of biphasic ^{18}F-FDG PET/CT imaging were plotted. The analysis showed that the diagnostic efficacy of metabolic parameters in distinguishing adenocarcinoma from squamous cell carcinoma ranged from high to low was SUV_{peak} (AUC = 0.727, 95%:0.638–0.815), SUV_{max} (AUC = 0.708, 95%:0.617–0.799), $dpSUV_{max}$ (AUC = 0.699, 95%:0.608–0.791), $dpSUV_{peak}$ (AUC = 0.698, 95%: 0.607–0.790), TLG (AUC = 0.695, 95%: 0.604–0.786), dpTLG (AUC = 0.692, 95%: 0.600–0.784), SUV_{mean} (AUC = 0.690, 95%: 0.597–0.782), $dpSUV_{mean}$ (AUC = 0.687, 95%: 0.593–0.781), $dpSUV_{min}$ (AUC = 0.680, 95%: 0.586–0.774), SUV_{min} (AUC = 0.676, 95%: 0.597–0.782), and MTV (AUC = 0.657, 95%: 0.562–0.752). This is similar to the conclusion of previous studies [30,31] that delayed phase (2 h after injection) ^{18}F-FDG PET/CT does not improve the diagnostic efficiency in distinguishing AC from SCC in the early phase (1 h after injection). This may be related to the significant overlap of metabolic parameters between squamous cell carcinoma and lung adenocarcinoma. Theoretically, tumor cells' metabolic activity, cell proliferation, and invasion abilities in cell carcinoma differ from those of lung adenocarcinoma. The changing trends of ^{18}F-FDG uptake by both cell types differ with time. However, owing to the large overlap, the metabolic parameters of ^{18}F-FDG PET/CT in the delayed period did not significantly improve the diagnostic efficacy for distinguishing lung AC from SCC.

This study has some limitations. First, we studied only the two most common pathological subtypes of lung cancer. Second, delayed images were acquired 2 h after the injection of ^{18}F-FDG, which is a commonly used acquisition time in several studies. In addition, this was a single-center retrospective study, and there were differences in sex ratios between the AC and SCC cohorts, which may have introduced a selection bias. To address the above issues, further studies should be conducted on more pathological types, such as adenosquamous, large, and giant cell carcinoma. Secondly, because different delayed collection times produce different results, we believe the delay can be fixed. Finally, for a single-center retrospective study with sex bias, we suggest that this problem can be avoided

by using a larger sample size and a multicenter study.

5. Conclusion

Squamous cell carcinoma of the lung has a higher mean MTV, SUV_{max}, TLG, SUV_{peak}, SUV_{mean}, SUV_{min}, $dpSUV_{peak}$, $dpSUV_{mean}$, $dpSUV_{min}$, $dpSUV_{max}$, and dpTLG of the tumor than AC; therefore, these parameters can help differentiate between SCC and AC. However, the metabolic parameters of the delayed-phase (2 h after injection) ^{18}F-FDG PET/CT did not improve the diagnostic efficacy in distinguishing lung AC from SCC. Therefore, conventional dual-phase ^{18}F-FDG PET/CT is not recommended. This study has many limitations. Next, we will increase the sample size to avoid selection bias and make our results more objective and credible. In addition, we will follow-up with the patients and analyze the relationship between metabolic parameters and survival.

Author contribution statement

Xue Liu; Qiao Zou: Conceived and designed the experiments; Analyzed and interpreted the data; Performed the experiments; Wrote the paper. Cailiang Gao: Conceived and designed the experiments. Yu Sun: Performed the experiments; Analyzed and interpreted the data. Huiting Liu: Contributed reagents, materials, analysis tools or data.

Data availability statement

Data included in article/supp. material/referenced in article.

Funding statement

This work was supported by Wanzhou District Science and Health Union Medical Project (Grant No. wzstc-kw2020020), and Scientific research project of Chongqing University Three Gorges Hospital (Grant No. 2022YJKYXM-046), Chongqing, China.

Ethics approval and consent to participate

Ethics approval and consent to participate were taken from our institute ethical committee (Chongqing University Three Gorges Hospital) with written informed consents were waived being a retrospective study.

Declaration of competing interest

The authors declare that they have no known competing financial interests or personal relationships that could have appeared to influence the work reported in this paper.

Acknowledgement

Not applicable.

References

[1] R. Maconachie, T. Mercer, N. Navani, G. McVeigh, Lung cancer: diagnosis and management: summary of updated NICE guidance, BMJ 364 (2019) l1049, https://doi.org/10.1136/bmj.l1049.
[2] T.K. Hayes, M. Meyerson, Molecular portraits of lung cancer evolution, Nature Publishing Group UK London 616 (2023) 435–436, https://doi.org/10.1038/d41586-023-00934-0.
[3] Y. Zhao, Y. Gao, X. Xu, J. Zhou, H. Wang, Multi-omics analysis of genomics, epigenomics and transcriptomics for molecular subtypes and core genes for lung adenocarcinoma, BMC Cancer 21 (1) (2021) 257, https://doi.org/10.1186/s12885-021-07888-4.
[4] D. Planchard, S.T. Popat, K. Kerr, S. Novello, E.F. Smit, C. Faivre-Finn, et al., Metastatic non-small cell lung cancer: ESMO Clinical Practice Guidelines for diagnosis, treatment and follow-up, Ann. Oncol. 29 (2018) iv192–iv237, https://doi.org/10.1093/annonc/mdy275.
[5] G. Scagliotti, N. Hanna, F. Fossella, K. Sugarman, J. Blatter, P. Peterson, et al., The differential efficacy of pemetrexed according to NSCLC histology: a review of two Phase III studies, Oncol. 14 (3) (2009) 253–263, https://doi.org/10.1634/theoncologist.2008-0232.
[6] D.S. Ettinger, D.E. Wood, D.L. Aisner, W. Akerley, J.R. Bauman, A. Bharat, et al., Non–small cell lung cancer, version 3.2022, NCCN clinical practice guidelines in oncology, J. Natl. Compr. Cancer Netw. 20 (5) (2022) 497–530, https://doi.org/10.6004/jnccn.2022.0025.
[7] F. Yang, W. Chen, H. Wei, X. Zhang, S. Yuan, X. Qiao, et al., Machine learning for histologic subtype classification of non-small cell lung cancer: a retrospective multicenter radiomics study, Front. Oncol. 10 (2021), 608598, https://doi.org/10.3389/fonc.2020.608598.
[8] D.S. Surasi, P. Bhambhvani, J.A. Baldwin, S.E. Almodovar, J.P. O'Malley, 18F-FDG PET and PET/CT patient preparation: a review of the literature, J. Nucl. Med. Technol. 42 (2014) 5–13, https://doi.org/10.2967/jnmt.113.132621.
[9] Y.-.H. Qu, N. Long, C. Ran, J. Sun, The correlation of 18F-FDG PET/CT metabolic parameters, clinicopathological factors, and prognosis in breast cancer, Clin. Transl. Oncol. 23 (2021) 620–627, https://doi.org/10.1007/s12094-020-02457-w.
[10] H. Sari, C. Mingels, I. Alberts, J. Hu, D. Buesser, V. Shah, et al., First results on kinetic modelling and parametric imaging of dynamic 18F-FDG datasets from a long axial FOV PET scanner in oncological patients, Eur. J. Nucl. Med. Mol. Imag. 49 (2022) 1997–2009, https://doi.org/10.1007/s00259-021-05623-6.
[11] M. Nakajo, M. Jinguji, M. Aoki, A. Tani, M. Sato, T. Yoshiura, The clinical value of texture analysis of dual-time-point 18 F-FDG-PET/CT imaging to differentiate between 18 F-FDG-avid benign and malignant pulmonary lesions, Eur. Radiol. 30 (2020) 1759–1769, https://doi.org/10.1007/s00330-019-06463-7.
[12] E. Okazaki, H. Seura, Y. Hasegawa, T. Okamura, H. Fukuda, Prognostic value of the volumetric parameters of dual–time-point 18F-FDG PET/CT in non–small cell lung cancer treated with definitive radiation therapy, Am. J. Roentgenol. 213 (6) (2019) 1366–1373, https://doi.org/10.2214/AJR.19.21376.

[13] L. Pang, X. Bo, J. Wang, C. Wang, Y. Wang, G. Liu, et al., Role of dual-time point 18 F-FDG PET/CT imaging in the primary diagnosis and staging of hilar cholangiocarcinoma, Abdominal Radiology 46 (2021) 4138–4147, https://doi.org/10.1007/s00261-021-03071-2.
[14] I.S. Ahmed, S.M. El Gaafary, R.Z. Elia, R.S. Hussein, FDG-PET/CT in predicting aggressiveness of rectal cancer, Egyptian Journal of Radiology and Nuclear Medicine 52 (2021) 275, https://doi.org/10.1186/s43055-021-00656-1.
[15] A. Shi, J. Wang, Y. Wang, G. Guo, C. Fan, J. Liu, Predictive value of multiple metabolic and heterogeneity parameters of 18F-FDG PET/CT for EGFR mutations in non-small cell lung cancer, Ann. Nucl. Med. 36 (2022) 393–400, https://doi.org/10.1007/s12149-022-01718-8.
[16] Y. Ren, J. Liu, L. Wang, Y. Luo, X. Ding, A. Shi, et al., Multiple metabolic parameters and visual assessment of 18F-FDG uptake heterogeneity of PET/CT in advanced gastric cancer and primary gastric lymphoma, Abdominal Radiology 45 (2020) 3569–3580, https://doi.org/10.1007/s00261-020-02503-9.
[17] D. Wang, X. Zhang, H. Liu, B. Qiu, S. Liu, C. Zheng, et al., Assessing dynamic metabolic heterogeneity in non-small cell lung cancer patients via ultra-high sensitivity total-body [18F]FDG PET/CT imaging: quantitative analysis of [18F]FDG uptake in primary tumors and metastatic lymph nodes, Eur. J. Nucl. Med. Mol. Imag. 49 (2022) 4692–4704, https://doi.org/10.1007/s00259-022-05904-8.
[18] K. Zhao, C. Wang, F. Shi, Y. Huang, L. Ma, M. Li, et al., Combined prognostic value of the SUVmax derived from FDG-PET and the lymphocyte-monocyte ratio in patients with stage IIIB-IV non-small cell lung cancer receiving chemotherapy, BMC Cancer 21 (2021) 66, https://doi.org/10.1186/s12885-021-07784-x.
[19] W. Yan, C. Sun, X. Ou, C. Hu, Prognostic value of pre-treatment FDG PET/CT SUVmax for metastatic lesions in de novo metastatic nasopharyngeal carcinoma following chemotherapy and locoregional radiotherapy, Cancer Imag. 23 (2023) 21, https://doi.org/10.1186/s40644-023-00536-z.
[20] X. Liao, M. Liu, R. Wang, J. Zhang, Potentials of non-invasive 18F-FDG PET/CT in immunotherapy prediction for non–small cell lung cancer, Front. Genet. 12 (2022), 810011, https://doi.org/10.3389/fgene.2021.810011.
[21] J. Zhou, S. Zou, S. Cheng, D. Kuang, D. Li, L. Chen, et al., Correlation between dual-time-point FDG PET and tumor microenvironment immune types in non-small cell lung cancer (NSCLC), Front. Oncol. 11 (2021), 559623, https://doi.org/10.3389/fonc.2021.559623.
[22] Y. Guo, H. Zhu, Z. Yao, F. Liu, D. Yang, The diagnostic and predictive efficacy of 18F-FDG PET/CT metabolic parameters for EGFR mutation status in non-small-cell lung cancer: a meta-analysis, Eur. J. Radiol. 141 (2021), 109792, https://doi.org/10.1016/j.ejrad.2021.109792.
[23] T.W.H. Meijer, M.G. Looijen-Salamon, J. Lok, M. van den Heuvel, B. Tops, J.H. Kaanders, et al., Glucose and glutamine metabolism in relation to mutational status in NSCLC histological subtypes, Thoracic Cancer 10 (2019) 2289–2299, https://doi.org/10.1111/1759-7714.13226.
[24] M. Ouyang, H. Xia, M. Xu, J. Lin, L. Wang, X. Zheng, et al., Prediction of occult lymph node metastasis using SUV, volumetric parameters and intratumoral heterogeneity of the primary tumor in T1-2N0M0 lung cancer patients staged by PET/CT, Ann. Nucl. Med. 33 (2019) 671–680, https://doi.org/10.1007/s12149-019-01375-4.
[25] L. de Geus-Oei, J.H.J.M. van Krieken, R.P. Aliredjo, P.F.M. Krabbe, C. Frielink, A.F.T. Verhagen, et al., Biological correlates of FDG uptake in non-small cell lung cancer, Lung Cancer 55 (2007) 79–87, https://doi.org/10.2967/jnmt.119.236109.
[26] I. Sarikaya, A. Sarikaya, Assessing PET parameters in oncologic 18F-FDG studies, J. Nucl. Med. Technol. 48 (2020) 278–282, https://doi.org/10.2967/jnmt.119.236109.
[27] K. Pahk, J.H. Chung, S. Kim, S.H. Lee, Predictive value of dual-time 18F-FDG PET/CT to distinguish primary lung and metastatic adenocarcinoma in solitary pulmonary nodule, Tumori Journal 104 (2018) 207–212, https://doi.org/10.1177/0300891618766203.
[28] R. Sa, H. Zhao, Y. Dai, F. Guan, The role of dual time point PET/CT for distinguishing malignant from benign focal 18F-FDG uptake duodenal lesions, Medicine 97 (2018), e12521, https://doi.org/10.1097/MD.0000000000012521.
[29] Y. Huang, Y. Huang, M. Ko, C. Hsu, C. Chen, Dual-time-point 18 F-FDG PET/CT in the diagnosis of solitary pulmonary lesions in a region with endemic granulomatous diseases, Ann. Nucl. Med. 30 (2016) 652–658, https://doi.org/10.1007/s12149-016-1109-4.
[30] M.M. Sathekge, A. Maes, H. Pottel, A. Stoltz, C. Van De Wiele, Dual time-point FDG PET/CT for differentiating benign from malignant solitary pulmonary nodules in a TB endemic area, S. Afr. Med. J. 100 (2010), https://doi.org/10.7196/samj.4082, 598-561.
[31] R.L. Barger Jr., K.R. Nandalur, Diagnostic performance of dual-time 18F-FDG PET in the diagnosis of pulmonary nodules: a meta-analysis, Acad. Radiol. 19 (2012) 153–158, https://doi.org/10.1016/j.acra.2011.10.009.